Available online at www.sciencedirect.com
ScienceDirect
Journal of the European Ceramic Society 29 (2009) 2807–2813
www.elsevier.com/locate/jeurceramsoc

In situ preparation of $CoFe_2O_4$–$Pb(ZrTi)O_3$ multiferroic composites by gel-combustion technique

A.R. Iordan [a], M. Airimioaiei [b], M.N. Palamaru [a], C. Galassi [b], A.V. Sandu [c], C.E. Ciomaga [d,*], F. Prihor [d], L. Mitoseriu [d], A. Ianculescu [e]

[a] *Faculty of Chemistry, Al. I. Cuza University, Iasi 700506, Romania*
[b] *ISTEC-CNR, Via Granarolo no. 64, I-48018 Faenza, Italy*
[c] *Romanian Inventors Forum, Iasi 700089, Romania*
[d] *Faculty of Physics, Al. I. Cuza University, Iasi 700506, Romania*
[e] *Faculty of Applied Chemistry and Materials Science, Polytechnics University of Bucharest, Gh. Polizu 1-7, Romania*

Received 21 January 2009; received in revised form 20 March 2009; accepted 31 March 2009
Available online 2 May 2009

Abstract

Diphase magnetoelectric composites of $CoFe_2O_4$–$Pb(ZrTi)O_3$ were prepared by citrate–nitrate combustion technique by using $Pb(Zr,Ti)O_3$ template powders obtained by the mixed oxide method. Pure diphase powder composites with a good crystallinity were obtained after calcination. The composition and purity were maintained after sintering at temperature of 1100 °C/2 h, which ensured limited reactions at interfaces, while by sintering at 1250 °C/2 h, some small amounts of secondary phases identified as nonstoichiometric ZrO_{2-x} resulted. The method allowed to produce diphase ceramics with homogeneous microstructures and a very good mixing of the two phases. The dielectric and magnetic investigation at room temperature confirmed the formation of composite ceramics with both dielectric and magnetic properties at room temperature, with permittivity and magnetization resulted as sum properties from the parent $Pb(Zr,Ti)O_3$ and ferrite phases.

Keywords: Electrical properties; Magnetic properties; Ferrites; PZT

1. Introduction

The multiferroics are functional materials combining several ferroic properties in the same phase. They exhibit simultaneously magnetic and ferroelectric order and a coupling between them.[1,2] The large interest in the magnetoelectric (ME) multiferroics is related to the technological potentiality of using the cross-correlation between the magnetic and electric properties in electronic devices. Apart from the properties of the parent phases (ferro-, anti-ferroelectricity and ferro-, antiferro-, ferri-magnetism), the ME effect adds a supplementary freedom degree in designing materials for new applications, opening the possibility to manipulate the magnetic properties through electric fields and *vice versa*. These properties give additional potentiality for applications in spintronics, multiple state memory elements or novel memory devices which might use electric and/or magnetic fields for read/write operations.[1,2] Following the general tendency of the microelectronic industry towards miniaturization and integration, finding materials with best properties in smaller volumes and combining more than one function in the same structure has become a very actual task. In spite the first ME phenomena were discovered in the 1960s, the expected breakthrough in the field of applications did not take place, particularly due to very low values found for the coupling coefficients.[3] In addition, serious limits in understanding the basic chemistry and physics related to these effects led to a reduced interest in the topic for around two decades. A true "revival of the magnetoelectric effect"[4] or "renaissance of the magnetoelectric multiferroics"[5] was only recently observed, which manifests by an impressive increasing of the number of publications in this field after 2000.[4] The main results concerning the fundamental aspects and multifunctional applications, as well as the problems

* Corresponding author at: Faculty of Physics, Al. I. Cuza University, Bv. Carol I, no 11, Iasi 700506, Romania. Tel.: +40 232201175; fax: +40 232201205.
E-mail address: cristina.ciomaga@uaic.ro (C.E. Ciomaga).

0955-2219/$ – see front matter © 2009 Elsevier Ltd. All rights reserved.
doi:10.1016/j.jeurceramsoc.2009.03.031

related to the new concepts in design, preparation, investigation and theoretical treatment of various ME structures in single-phase and composites, are presented in many recent reviews.[3,4,6,7]

Searching for two-phase composites was promoted by the reduced number of systems intrinsically showing the ME coupling and by practical needs, due to low values of the ME coefficient (of the order of 1–20 mV/cm Oe) found in single-phase materials and by the cryogenic temperatures needed for the ME coupling.[3] The ME effect is realised in composites on the concept of *product property*.[8] According to this principle, a suitable combination of two phases such as piezomagnetic or magnetostrictive and piezoelectric phases can yield a desirable ME property. The conceptual conditions for the ME effect in composites were pointed out by Boomgaard,[9] as following: (i) the individual phases should be in chemical equilibrium, (ii) no mismatch between grains, (iii) high values for the magnetostriction coefficient of the piezomagnetic or magnetostrictive phase and of the piezoelectric coefficient of the ferroelectric phase, (iv) no leak of the accumulated charges through the phases. Following this principle, various ME composites have been prepared, consisting by ferroelectrics as $BaTiO_3$, $Pb(ZrTi)O_3$, $BaPbTiO_3$, $Bi_4Ti_3O_{12}$ while Ni, Co, Mg, (Ni, Zn), (Ni,Co,Mn), ferrites as magnetic phase were employed, in particulate, laminated or multilayer film structures, as presented in the recent review of Nan et al.[10] The main advantages to produce sintered ME composites are related to the easy and cheap fabrication and to the possibility to control the molar ratio of phases, grain size of each phase and densification by using good quality powders, a good mixing of the two phases and appropriate sintering strategy. However, in the bulk composites, a large variety of dielectric and ME properties were reported for similar systems and even for the same composition. In addition, high dielectric losses ($\tan\delta \gg 1$) at room temperature were normally found.[10–16] These were considered as originating mainly from microstructural effects and to the presence of secondary phases formed during the sintering step. In the large majority of publications reporting data on composite ceramics, a direct mechanical mixing of the ferroelectric and magnetic phases separately prepared was employed for producing the composite. This simply mixing was considered a reason for the obtained low ME effect, as result of poor control of the mechanical defects and to low percolation threshold limits.

In our previous works[13,14] concerning $(Ni,Zn)Fe_2O_4$–$BaTiO_3$ ceramic composites, it was demonstrated that the method of in situ synthesis ensures a better mixing and much more homogeneous microstructures, leading to serious reduction of the dielectric losses. An in situ sol–gel method followed by a conventional sintering was also used by Wu et al.[17] resulting in homogeneous composite ceramic microstructures with $NiFe_2O_4$ grains well dispersed in a PZT matrix. Thus, it is expected that a better control of the microstructure and connectivity can be achieved by in situ processing of the ferroelectric–magnetic composite. In the present paper, the method of producing in situ $CoFe_2O_4$–$Pb(Zr,Ti)O_3$ composites by gel-combustion method was adopted.

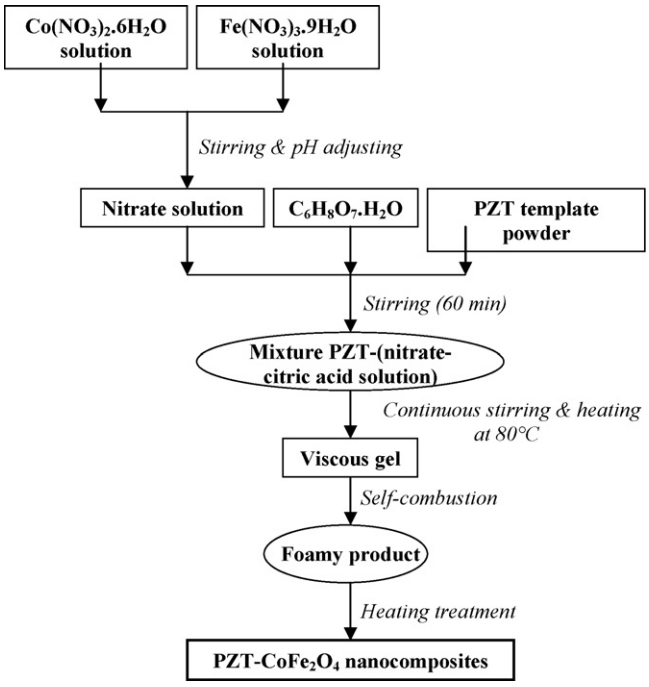

Fig. 1. Flowchart of the composite powder preparation.

2. Sample preparation and experimental details

$Pb(Zr_{0.47}Ti_{0.53})O_3$ (PZT) ($\rho_{th} = 7.952$ g/cm^3) template powders were firstly prepared by a conventional solid state reaction method by using reagent grade PbO (Aldrich 211907, purity 99.9%), ZrO_2 (MEL SC101), and TiO_2 (Degussa P25). The precursors were ball milled with zirconia milling media in water for 48 h, freeze dried, sieved to 250 μm and calcined at 800 °C/4 h. The calcined powder was wet milled in ethanol (100 h), then dried and sieved. The mean diameter (d_{50}) of the PZT calcined powder was 0.71 μm and the specific surface area of 2.67 m^2/g.

$CoFe_2O_4$ (CF) and xCF–$(1-x)$PZT composite powders ($x = 10$, 20, 30 wt.%) were prepared by citrate–nitrate combustion method, following a similar procedure as for obtaining $CoMn_xFe_{2-x}O_4$, previously reported.[18,19] The synthesis procedure of the composite powders is described in the flowchart shown in Fig. 1. Stoichiometric amounts of cobalt (II) nitrate hexahydrate ($Co(NO_3)_2{\cdot}6H_2O$ p.a. Merck) and iron (III) nitrate nonahydrate ($Fe(NO_3)_3{\cdot}9H_2O$, 99.9%, Aldrich) solutions were mixed. The pH of the obtained solution was increased to 7 by the addition of ammonium hydroxide (25% NH_3 in H_2O p.a. Fluka). Finally, the nitrate solutions were mixed with aqueous citric acid $C_8H_{12}O_7$ (≥99.5% Sigma–Aldrich). The molar ratio of total metal ions to citric acid was 1:1 in the solution. The mixtures PZT–(nitrate/citric acid solution) were stirred for 60 min and then they were heated at 80 °C, under continuous stirring. After the evaporation of water excess, a highly viscous gel has been obtained. Subsequently, the gel was ignited at 300 °C to evolve the undesirable gaseous products, resulting in the formation of a foamy powder containing the composite precursor. To complete the ferrite formation onto the PZT templates, the powder mixture was calcined at 500 °C/8 h resulting in fine composite powders of xCF–$(1-x)$PZT ($x = 0.10$, 0.20 and 0.30).

The composite powders were grounded, and then cold isostatically pressed at 300 MPa into discs of 30 mm diameter (green bodies). The samples were sintered either at 1100 °C/2 h or at 1250 °C/2 h, in Pb atmosphere maintained by a $PbZrO_3$ source in a closed Al_2O_3 crucible. After sintering the ceramic pellets were superficially polished to remove the surface layers.

The phase formation of the $CoFe_2O_4$ ferrite onto the PZT templates was checked by using a Fourier transform infrared (FTIR) spectra, recorded in the range 4000 cm^{-1} to 400 cm^{-1} with 2 cm^{-1} resolution on a Jasco 660 plus FTIR spectrophotometer using the KBr pellet technique. X-ray diffraction measurements at room temperature for investigating the formation of the perovskite and spinel phases in the composite powders and in the sintered pellets were performed with a SHIMADZU XRD 6000 diffractometer using Ni-filtered CuKα radiation (λ = 1.5418 Å), with a scan step of 0.02° and a counting time of 1 s/step, for 2θ ranging between 20° and 80°. The microstructure of the composite powders and of the sintered ceramics was examined by using a scanning electron microscope (SEM) coupled with energy-dispersive X-ray spectroscopy (EDX) (VEGA/TESCAN instrument). The electrical measurements were performed on parallel-plate capacitor configuration, by applying Pd–Ag electrodes on the polished surfaces of the sintered ceramic disks. The complex impedance in the frequency domain (20 Hz to 2 MHz) at room temperature was determined by using an impedance bridge type Agilent E4980A Precision LCR Meter. The magnetic properties at room temperature were determined under magnetic fields up to 14 kOe with a Vibrating Sample Magnetometer MicroMag™ VSM model 3900 (Princeton Measurements Co.).

3. Results and discussions

The decomposition reactions of the starting composition are as follows:

$$Co(NO_3)_2{\cdot}6H_2O = CoO + NO_2 + NO + O_2 + 6H_2O \quad (1)$$

$$Fe(NO_3)_3 \cdot 9H_2O = \frac{1}{2}Fe_2O_3 + \frac{3}{2}NO_2 + \frac{3}{2}NO + \frac{3}{2}O_2 + 9H_2O \quad (2)$$

$$C_8H_{12}O_7 + \tfrac{15}{2}O_2 = 8CO_2 + 6H_2O \quad (3)$$

From the above reactions it has been understood that the decomposition of citric acid is highly exothermic, aiding the decomposition of nitrates salts into the desired products at a faster rate and with low external-energy consumption. Citric acid is a suitable organic fuel because it is cheap and readily available commercially and its decomposition generates high temperature during the combustion process, leading to the full formation of the ferrite phase under mild external conditions. The overall combustion reaction in air resulting in the ferrite

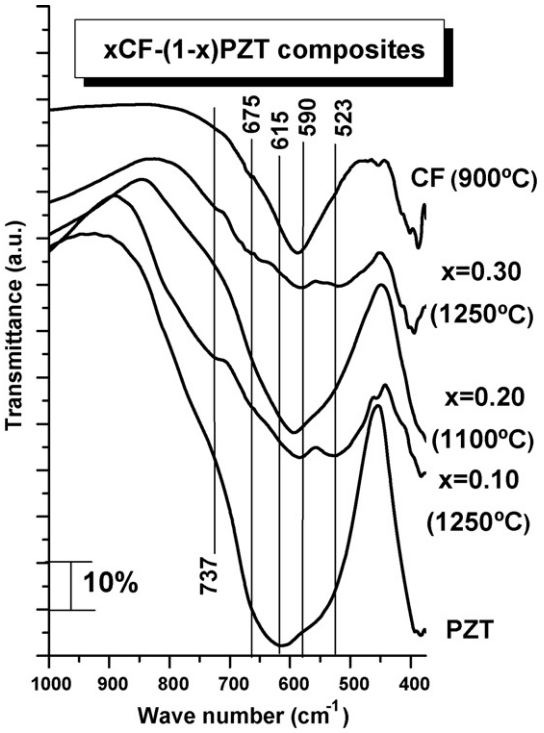

Fig. 2. FTIR spectra of the combustion synthesized xCF–$(1-x)$PZT composites.

phase formation is described by the reaction:

$$Co(NO_3)_2 \cdot 6H_2O + 2Fe(NO_3)_3 \cdot 9H_2O + 3C_8H_{12}O_7 + \tfrac{37}{2}O_2 = CoFe_2O_4 + 4NO_2 + 4NO + 24CO_2 + 42H_2O \quad (4)$$

In order to confirm the formation of the CF spinel phase onto the PZT powder templates, the FTIR spectra of the composite powders were collected. Fig. 2 shows the FTIR spectra of the combustion synthesized xCF–$(1-x)$PZT composites recorded in the range between 400 and 1000 cm^{-1}. The spectra elucidate the position of cations in the crystal structure with oxygen ions and their vibration modes, which represents the various ordering positions of the structural characteristics. The metal cations in the spinel ferrite structure AB_2O_4 are situated in two different sub-lattices namely tetrahedral (A-sites) and octahedral (B-sites), according to the geometric configuration of the nearest oxygen ion neighbors. The absorption bands around 667 and 603 cm^{-1} present in all the ferrite spectra are assigned to the stretching vibrations of M–O (M = Fe, Co) bands in $CoFe_2O_4$ compounds, as reported by Waldron.[20] The band around 600 cm^{-1} is attributed to stretching vibration of tetrahedral complexes and the band around 400 cm^{-1} to that of the octahedral complexes. Due to the stretching vibration of Fe^{3+}–O^{2-} for tetrahedral sites,[21] all the systems containing the ferrite show an absorption band at ~590 cm^{-1}. The presence of Co in tetrahedral centers is proved by the occurrence of the absorption maximum at ~675 cm^{-1}, due to the vibration of CoO_4.[22] The bands at ~675 cm^{-1} and at ~590 cm^{-1} present in the spectra of the calcined powders indicate the formation of metal oxide, also confirmed by the XRD analysis as being a spinel single phase. Vibration spectroscopic techniques,

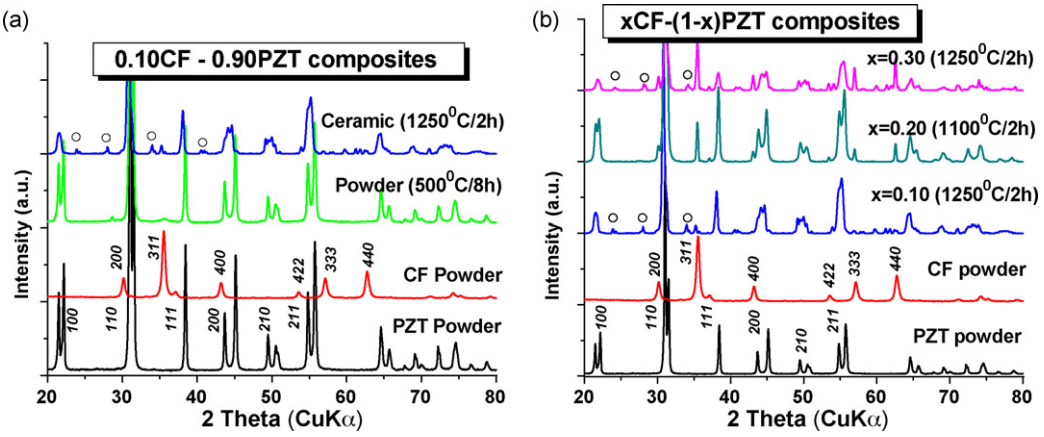

Fig. 3. XRD pattern of the $x CoFe_2O_4$–$(1-x)Pb(Zr,Ti)O_3$ composites and of the parent phases of $Pb(Zr,Ti)O_3$ and $CoFe_2O_4$: (a) $x = 0.10$ calcined powder and ceramic sintered at 1250 °C/2 h; (b) sintered ceramics with various compositions. Note the absence of secondary phases for the calcined powders and for the ceramics sintered at 1100 °C/2 h.

such as infrared spectroscopy, are also useful tools for detecting structural changes in PZT and it was used to monitor the perovskite phase formation during the syntheses. PZT crystallizes in a perovskite structure ABO_3, where A-sites are occupied by Pb^{2+} ions, whereas Zr^{4+} and Ti^{4+} ions randomly occupy the B-sites and the central Zr^{4+} or Ti^{4+} ions are surrounded by six oxygen ions in octahedral coordination.[23] The ν_1 stretching modes (Ti–O and Zr–O stretch) occur at wave numbers above 400 cm^{-1}.[24] For the $PbZr_{0.50}Ti_{0.50}O_3$, the modes at ~660 cm^{-1} and ~615 cm^{-1} were assigned to the ν_1 Ti–O stretching vibrations and the modes at ~770 cm^{-1} and ~547 cm^{-1} to the Zr–O stretching vibrations.[25] According to these interpretations, for our PZT templates, the shoulders at ~737 cm^{-1} and 523 cm^{-1} may be associated with the Zr–O stretching mode, while the shoulder at ~675 cm^{-1} and the maximum at ~615 cm^{-1} to the Ti–O stretching mode. The transformation of the shoulder at ~523 cm^{-1} attributed to the Zr–O bond in PZT in a well-defined maximum after the thermal treatment at 1250 °C might be originated in the formatting of small amounts of Zr-rich secondary phases. The XRD analysis presented in the following (Fig. 3) indicates the presence of small amounts of ZrO_{2-x} nonstoichiometric oxide in the ceramics sintered at higher temperature (1250 °C), which supports such an interpretation.

The phase purity after the calcination step and after sintering was checked by XRD investigation. The XRD patterns confirmed the successful formation of a diphase composite for each composition, formed by the spinel $CoFe_2O_4$ and $Pb(ZrTi)O_3$ perovskite phases in the nominal proportion, both after the calcination step and after the sintering in bulk at 1100 °C/2 h (Fig. 3). The increasing sintering temperature to 1250 °C aimed to lead to a better densification, results in the formation of some small amount of the nonstoichiometric ZrO_{2-x}, as demonstrated by the presence of small maxima around $2\theta \sim 24°$, ~28° and ~34°, besides the main peaks of the parent phases (Fig. 3a–b). This residual phase resulted most probably from the use of the $PbZrO_3$ covering powder during sintering for compensating the Pb-evaporation was fully eliminated after polishing the ceramic surfaces. Therefore, by sintering in the range of 1100–1250 °C, both a good densification and a minimization of the secondary phases can be realized. As expected, a better crystallization is

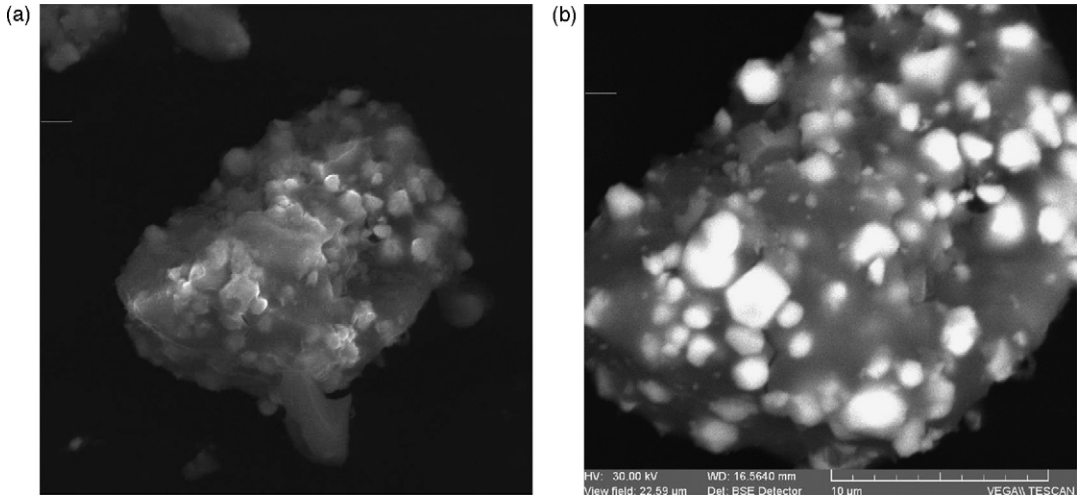

Fig. 4. SEM images of CF–PZT in situ prepared composite powder after the calcination step: (a) secondary electron image; (b) backscattering image (white: PZT, grey: CF).

obtained after thermal treatment at higher temperatures. The crystallite size determined by the Debye–Scherrer equation are: 150–180 nm for PZT phase and of 60–80 nm for CF component in the powder composites. Their size remains almost unchanged for the PZT phase, but strongly increases to ~250 nm for the ferrite component in the ceramic product. Since well-crystallized PZT powders were used as template for the in situ preparation of the powder composites, the subsequent thermal treatments for promoting the CF formation practically did not change the crystallization of the PZT component. For various compositions of the xCF–$(1-x)$PZT ceramics sintered at the same temperature, the proportion of the two phases determined from the relative peak intensity ratios of the parent phases were very close to the nominal ones.

The SEM images of the $CoFe_2O_4$–$Pb(ZrTi)O_3$ powder composite after the calcination step are presented in Fig. 4, where both secondary electron image (Fig. 4a) and backscattering image (Fig. 4b) are shown, demonstrating that a very good mixing of the two phases resulted by this method of in situ processing. The backscattering contrast (Fig. 4b) allow to better distinguishing between the two different phases, since the yield of the collected backscattered electrons increases monotonically with the specimen's atomic number (the white grains were identified as PZT and the darker ones as CF). In addition, due to the self-combustion high energy, a partial de-aggregating of the PZT blocks was also achieved. Particles of 1–2 μm beside finer ones below 400 nm for the PZT phase are found in the composite after calcination (Fig. 4b). This resulted in a very good mixing of the two phases into the ceramic body, as shown in Fig. 5(a and b), where both components are rather homogeneous, with average grain size of 10–15 μm for $CoFe_2O_4$ and of 1–4 μm for the $Pb(ZrTi)O_3$ phase. As observed, the ferrite tends to form larger aggregates dispersed into the PZT matrix composed of smaller grains (Fig. 5b) in the sintered body.

The dielectric properties of the xCF–$(1-x)$PZT ceramic composites ($x=0$, 0.10 and 0.30) sintered at 1250 °C/2 h were checked as a function of frequency in the range of 10^3 to 2×10^6 Hz, at room temperature and they are shown in Fig. 6. The complex impedance plot (Fig. 6a) demonstrates a good homogeneity of the dielectric and conductive properties of the sintered composites. The impedance spectrum is characterized by single semicircular arcs, whose pattern changes with composition, indicating a modification of the resistance/reactance ratio when increasing the ferrite addition x. A shift of the semicircle center towards the origin of the complex plane plot takes place as result of the increasing dc-conductivity when higher the ferrite concentration. The bulk resistivity of the composites sintered at the same temperature of 1250 °C/2 h decreases from 11.5×10^6 Ω (for $x=0.10$) to 6×10^6 Ω ($x=0.30$). As result, the losses are also higher when increases the ferrite addition, as shown in Fig. 6c. Losses above unity are characteristic for frequencies below 1 kHz for the composition $x=0.30$. For all the compositions, the losses are strongly reducing with increasing frequency (having values below 10% for frequencies above 10^4 Hz for $x=0.10$ and above 2×10^5 Hz for $x=0.30$ compositions). Losses above unity were commonly reported for similar ferroelectric–magnetic composites, particularly at low frequencies and high temperatures and this behavior seems to be intrinsic to such dielectric–magnetic composites as a result of the uncompensated space charges at the hetero-interfaces giving rise to Maxwell–Wagner polarization.[3,4,6,7]

The permittivity vs. frequency for the xCF–$(1-x)$PZT ceramic composites ($x=0$, 0.10 and 0.30) is represented in Fig. 6b. If for the pure PZT ceramic, values of permittivity of $\varepsilon_r\sim550$ are observed together with a few piezoelectric resonance jumps at $\sim2\times10^4$, 2×10^5, 4×10^5, 5×10^5, 10^6 Hz, such effects disappeared in the composites and a monotonic reduction of the permittivity with frequency is observed. Both composites presented here have dielectric constant below 200. Their permittivity still decreases and saturates at 2×10^6 Hz to the values of $\varepsilon_r\sim125$ for $x=0.10$ and $\varepsilon_r\sim25$ for $x=0.30$. Similar dielectric properties were reported for PZT–Ni ferrite composites sintered by spark plasma sintering[26] and for PZT–(Ni,Zn) ferrite ceramics prepared by powder-in-sol precursor hybrid processing route.[27] In order to understand the contributions to the dielectric losses, the reasons for the strong reduction of the permittivity and the lack of piezoelectric resonance contributions in composites, a detailed dielectric study comprising a large frequency range and at various temperatures will be further performed. As a general effect, by

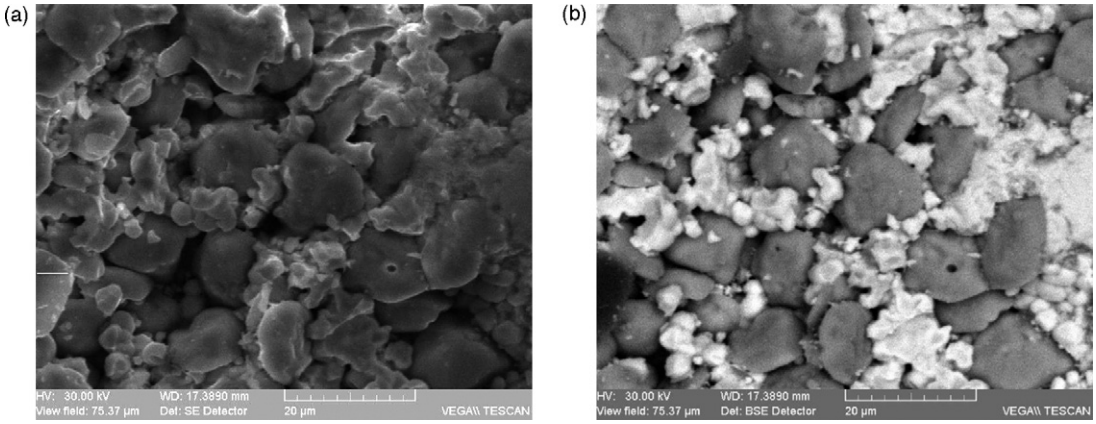

Fig. 5. SEM micrographs of the sintered composite CF–PZT ceramic: (a) secondary electron image; (b) backscattering image showing the dissimilar two phases (white: PZT, grey: CF grains).

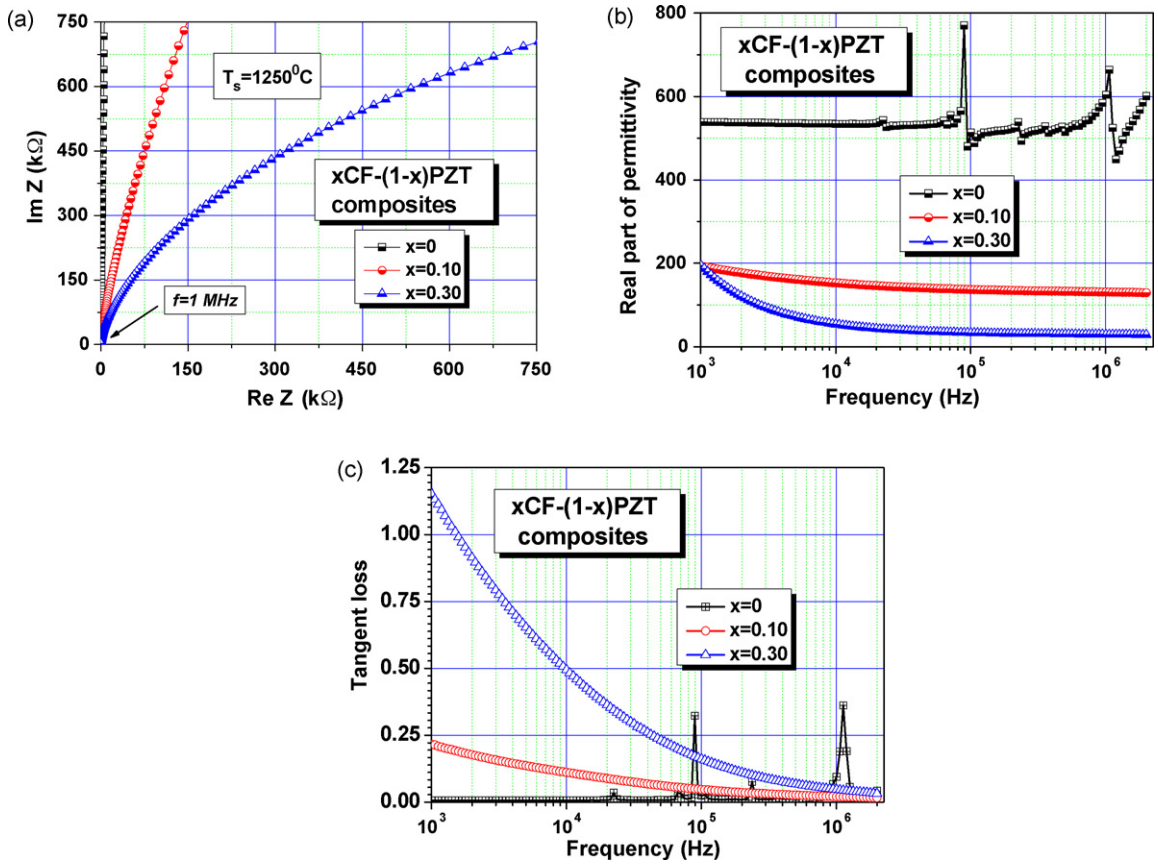

Fig. 6. Dielectric properties of the xCF–$(1-x)$PZT composites with $x = 0$, 0.10 and 0.30 at room temperature: (a) complex impedance plot; (b) real part of permittivity vs. frequency; (c) tangent loss vs. frequency.

comparison with the dielectric characteristics of particulate composites prepared by simple mixing of the two parent phases for which high losses (sometimes tan δ: tens or hundreds), multiple relaxations in kHz range and very small permittivity or conductive properties[3,4,7,10] the in situ prepared composites,[17,26,27] including the present ones, demonstrate their superior dielectric properties as a result of their much improved microstructures (better phase intermixing, lack of secondary phases and reduced porosity). Comparative with the most recent reported similar composites prepared by in situ processing, the proposed gel-combustion method gave rise to: (i) more homogeneous ferrite grain distribution within the ferroelectric matrix and more homogeneous electrical properties within the ceramic volume than reported in $NiFe_2O_4$–PZT composites prepared by sol–gel followed by solid state reaction[17] and (ii) much higher permittivity and lower losses at the same frequency than reported for $(Ni,Zn)Fe_2O_4$–PZT ceramics prepared by powder-in-sol precursor hybrid processing route.[27]

The magnetic hysteresis loops M(H) at room temperature (Fig. 7) show the presence of the ordered magnetic structure derived from the unbalanced antiparallel spins as in the pure $CoFe_2O_4$ system. As a consequence of the "sum property"[3,8] and to interface effects, a reduction of the saturation magnetization to ~30 emu/g ($x = 0.10$) and ~40 emu/g ($x = 0.30$) from the values reported for pure $CoFe_2O_3$ is noticed.[18]

The present investigations demonstrate the in situ obtaining of ceramic composite by gel-combustion method with high homogeneity of the two parent phases (concerning the grain size distribution and similar shape), better phase intermixing and good densification with reduced secondary reactions at the interfaces. Therefore, valuable dielectric and magnetic properties at room temperature were obtained, with permittivity and magnetization derived from ones of the parent PZT and ferrite phases. New results related to the lack of piezoelectric reso-

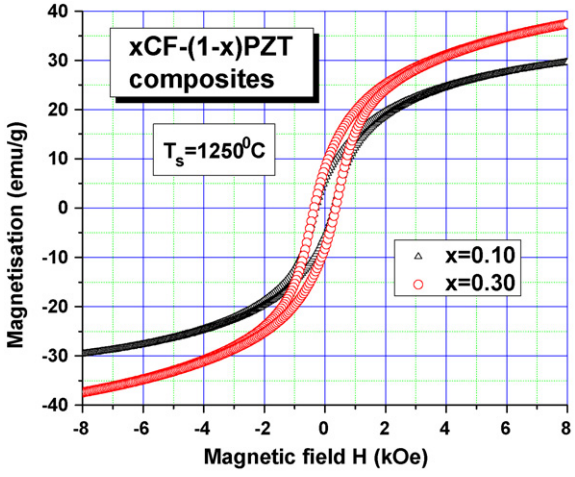

Fig. 7. Magnetic hysteresis loops at room temperature obtained for the xCF–$(1-x)$PZT composite ceramics with $x = 0.10$ and 0.30. *Note*: 1 emu/g = 1 m^2 A/kg.

nances in composites were noticed and these should be further investigated in detail.

4. Conclusions

$CoFe_2O_4$–$Pb(ZrTi)O_3$ magnetic–ferroelectric ceramic composites with limited reactions at interfaces were prepared by citrate–nitrate combustion technique by using $Pb(Zr,Ti)O_3$ template powders obtained by mixed oxide method. Pure diphase powder composites with a good crystallinity were obtained after the calcination step. The purity was maintained by sintering at temperature of 1100 °C/2 h. The increasing sintering temperature to 1250 °C/2 h resulted in a better densification, but also in the formation of some small amounts of secondary phases (mainly of ZrO_{2-x}), as demonstrated by the FTIR spectra and by the XRD investigation. The in situ preparation method resulted in homogeneous microstructures with a very good mixing of the two phases in the ceramic body, with lack of aggregation and formation of ferrite blocks, as normally found by simple mixing the ferrite and PZT powders, separately prepared. The dielectric and magnetic investigations at room temperature confirmed the formation of a composite with both dielectric and magnetic properties at room temperature, with permittivity and magnetization resulted as sum properties from the parent PZT and ferrite phases. By modifying the sintering parameters, the dielectric properties can be still further optimized.

References

1. Wood, V. E. and Austin, A. E., In *Magnetoelectric Interaction Phenomena in Crystals*, ed. A. J. Freeman and H. Schmid. Gordon and Breach, 1975.
2. Schmid, H., Multiferroic magnetoelectrics. *Ferroelectrics*, 1994, **162**, 317–338.
3. Ryu, J., Priya, S., Uchino, K. and Kim, H. E., Magnetoelectric effect in composites of magnetostrictive and piezoelectric materials. *J. Electroceram.*, 2002, **8**, 107–119.
4. Fiebig, M., Revival of the magnetoelectric effect. *J. Phys. D: Appl. Phys.*, 2005, **38**, R123–R152, and refs. herein.
5. Spaldin, N. A. and Fiebig, M., The renaissance of magnetoelectric multiferroics. *Science*, 2005, **309**, 391–392, and refs. herein.
6. Prellier, W., Singh, M. P. and Murugavel, P., The single-phase multiferroic oxides: from bulk to thin film. *J. Phys.: Condens. Matter*, 2005, **17**, R803–R832, and refs. herein.
7. Mitoseriu, L., Magnetoelectric phenomena in single-phase and composite systems. *Bol. Soc. Esp. Ceràm. e Vidrio*, 2005, **44**, 177–184, and refs. herein.
8. Van Suchetelene, J., Product properties: a new application of composite materials. *Philips Res. Rep.*, 1972, **27**, 28–37.
9. Van den Boomgaard, J. and Born, R. A. J., A sintered magnetoelectric composite material $BaTiO_3$–Ni $(Co,Mn)Fe_3O_4$. *J. Mater. Sci.*, 1978, **13**, 1538–1548.
10. Nan, C. W., Bichurin, M. I., Dong, S., Viehland, D. and Srinivasan, G., Multiferroic magnetoelectric composites: historical perspective, status, and future directions. *J. Appl. Phys.*, 2008, **103**, 031101.
11. Yu, Z. and Ang, C., Maxwell–Wagner polarization in ceramic composites $BaTiO_3$–$(Ni_{0.3}Zn_{0.7})Fe_{2.1}O_4$. *J. Appl. Phys.*, 2002, **91**, 794–797.
12. Qi, X., Zhou, J., Yue, Z., Gui, Z., Li, L. and Buddhudu, S., A ferroelectric ferromagnetic composite material with significant permeability and permittivity. *Adv. Funct. Mater.*, 2004, **9**, 920–926.
13. Mitoseriu, L., Buscaglia, V., Viviani, M., Buscaglia, M. T., Pallecchi, I., Harnagea, C. *et al.*, $BaTiO_3$–$(Ni_{0.5}Zn_{0.5})Fe_2O_4$ ceramic composites with ferroelectric and magnetic properties. *J. Eur. Ceram. Soc.*, 2007, **27**, 4379–4382.
14. Mitoseriu, L., Pallecchi, I., Buscaglia, V., Testino, A., Ciomaga, C. E. and Stancu, A., Magnetic properties of the $BaTiO_3$–$(Ni,Zn)Fe_2O_4$ multiferroic composites. *J. Magn. Magn. Mater.*, 2007, **316**, e603–e606.
15. Islam, R. A., Jiang, J., Bai, F., Viehland, D. and Priya, S., Correlation between structural deformation and magnetoelectric response in $(1-x)PbZr_{0.52}Ti_{0.48}O_3$–$xNiFe_{1.9}Mn_{0.1}O_4$ particulate composites. *Appl. Phys. Lett.*, 2007, **91**, 162905.
16. Tan, S. Y., Shannigrahi, S. R., Tan, S. H. and Tay, F. E. H., Synthesis and characterization of composite $MgFe_2O_4$–$BaTiO_3$ multiferroic system. *J. Appl. Phys.*, 2008, **103**, 094105.
17. Wu, D., Gong, W., Deng, H. and Li, M., Magnetoelectric composite ceramics of nickel ferrite and lead zirconate titanate via in situ processing. *J. Phys. D: Appl. Phys.*, 2007, **40**, 5002–5005.
18. Palamaru, M. N., Iordan, A. R., Aruxandei, C. D., Gorodea, I., Perianu, E. A., Dumitru, I. *et al.*, The synthesis of doped manganese cobalt ferrites by autocombustion technique. *J. Optoelectr. Adv. Mater.*, 2008, **10**(7), 1853–1856.
19. Cannas, C., Falqui, A., Musinu, A., Peddis, D. and Piccaluga, G., $CoFe_2O_4$ nanocrystalline powders prepared by citrate–gel methods: synthesis, structure and magnetic properties. *J. Nanopart. Res.*, 2006, **6**(2–3), 223–232.
20. Waldron, R. D., Infrared spectra of ferrites. *Phys. Rev.*, 1955, **99**, 1727.
21. Kalai Selvan, R., Augustin, C. O., JohnBerchmans, L. and Saraswathi, R., Combustion synthesis of $CuFe_2O_4$. *Mater. Res. Bull.*, 2003, **38**(1), 41–54.
22. Yu Chapskaya, A., Radishevskaya, N., Kasatskii, N., Lepakova, O., Naiborodenko Yu and Vereshchagin, V., The effect of composition and synthesis conditions on the structure of cobalt-bearing pigments of the spinel type. *Glass Ceram.*, 2005, **62**(11–12), 388–390.
23. Chang, K.-S., Hernandez, B. A., Fisher, E. and Dorhout, P. K., Sol–gel template synthesis and characterization of PT, PZ and PZT nanotubes. *J. Korean Chem. Soc.*, 2002, **46**(3), 242–251.
24. Perry, C. H., McCarthy, D. J. and Rupprecht, G., Dielectric dispersion of some perovskite zirconates. *Phys. Rev.*, 1965, **138**, A1537–A1538.
25. Guarany, C. A., Pelaio, L. H. Z., Araújo, E. B., Yukimitu, K., Moraes, J. C. S. and Eiras, J. A., Infrared studies of the monoclinic–tetragonal phase transition in Pb $(Zr,Ti)O_3$ ceramics. *J. Phys. Condens. Matter*, 2003, **15**, 4851–4857.
26. Jiang, Q. H., Shen, Z. J., Zhou, J. P., Shi, Z. and Nan, C. W., Magnetoelectric composites of nickel ferrite and lead zirconate titanate prepared by spark plasma sintering. *J. Eur. Ceram. Soc.*, 2007, **27**, 279–284.
27. Zhang, H., Or, S. W. and Chan, H. L. W., Multiferroic properties of $Ni_{0.5}Zn_{0.5}Fe_2O_4$–$PbZr_{0.53}Ti_{0.47}O_3$ ceramic composites. *J. Appl. Phys.*, 2008, **104**, 104109.